

## ADCY5 couples glucose to insulin secretion in human islets

Hodson, David J; Mitchell, Ryan K; Marselli, Lorella; Pullen, Timothy J; Gimeno Brias, Silvia; Semplici, Francesca; Everett, Katy L; Cooper, Dermot M F; Bugliani, Marco; Marchetti, Piero; Lavallard, Vanessa; Bosco, Domenico; Piemonti, Lorenzo; Johnson, Paul R; Hughes, Stephen J; Li, Daliang; Li, Wen-Hong; Shapiro, A M James; Rutter, Guy A

DOI:

[10.2337/db13-1607](https://doi.org/10.2337/db13-1607)

License:

Other (please specify with Rights Statement)

*Document Version*

Publisher's PDF, also known as Version of record

*Citation for published version (Harvard):*

Hodson, DJ, Mitchell, RK, Marselli, L, Pullen, TJ, Gimeno Brias, S, Semplici, F, Everett, KL, Cooper, DMF, Bugliani, M, Marchetti, P, Lavallard, V, Bosco, D, Piemonti, L, Johnson, PR, Hughes, SJ, Li, D, Li, W-H, Shapiro, AMJ & Rutter, GA 2014, 'ADCY5 couples glucose to insulin secretion in human islets', *Diabetes*, vol. 63, no. 9, pp. 3009-21. <https://doi.org/10.2337/db13-1607>

[Link to publication on Research at Birmingham portal](#)

### **Publisher Rights Statement:**

© 2014 by the American Diabetes Association. Readers may use this article as long as the work is properly cited, the use is educational and not for profit, and the work is not altered.

### **General rights**

Unless a licence is specified above, all rights (including copyright and moral rights) in this document are retained by the authors and/or the copyright holders. The express permission of the copyright holder must be obtained for any use of this material other than for purposes permitted by law.

- Users may freely distribute the URL that is used to identify this publication.
- Users may download and/or print one copy of the publication from the University of Birmingham research portal for the purpose of private study or non-commercial research.
- User may use extracts from the document in line with the concept of 'fair dealing' under the Copyright, Designs and Patents Act 1988 (?)
- Users may not further distribute the material nor use it for the purposes of commercial gain.

Where a licence is displayed above, please note the terms and conditions of the licence govern your use of this document.

When citing, please reference the published version.

### **Take down policy**

While the University of Birmingham exercises care and attention in making items available there are rare occasions when an item has been uploaded in error or has been deemed to be commercially or otherwise sensitive.

If you believe that this is the case for this document, please contact [UBIRA@lists.bham.ac.uk](mailto:UBIRA@lists.bham.ac.uk) providing details and we will remove access to the work immediately and investigate.

David J. Hodson,<sup>1</sup> Ryan K. Mitchell,<sup>1</sup> Lorella Marselli,<sup>2</sup> Timothy J. Pullen,<sup>1</sup> Silvia Gimeno Brias,<sup>1</sup> Francesca Semplici,<sup>1</sup> Katy L. Everett,<sup>3</sup> Dermot M.F. Cooper,<sup>3</sup> Marco Bugliani,<sup>2</sup> Piero Marchetti,<sup>2</sup> Vanessa Lavallard,<sup>4</sup> Domenico Bosco,<sup>4</sup> Lorenzo Piemonti,<sup>5</sup> Paul R. Johnson,<sup>6,7,8</sup> Stephen J. Hughes,<sup>6,7,8</sup> Daliang Li,<sup>9</sup> Wen-Hong Li,<sup>9</sup> A.M. James Shapiro,<sup>10</sup> and Guy A. Rutter<sup>1</sup>



# ADCY5 Couples Glucose to Insulin Secretion in Human Islets

Diabetes 2014;63:3009–3021 | DOI: 10.2337/db13-1607

**Single nucleotide polymorphisms (SNPs) within the *ADCY5* gene, encoding adenylate cyclase 5, are associated with elevated fasting glucose and increased type 2 diabetes (T2D) risk. Despite this, the mechanisms underlying the effects of these polymorphic variants at the level of pancreatic  $\beta$ -cells remain unclear. Here, we show firstly that *ADCY5* mRNA expression in islets is lowered by the possession of risk alleles at rs11708067. Next, we demonstrate that *ADCY5* is indispensable for coupling glucose, but not GLP-1, to insulin secretion in human islets. Assessed by in situ imaging of recombinant probes, *ADCY5* silencing impaired glucose-induced cAMP increases and blocked glucose metabolism toward ATP at concentrations of the sugar  $>8$  mmol/L. However, calcium transient generation and functional connectivity between individual human  $\beta$ -cells were sharply inhibited at all glucose concentrations tested, implying additional, metabolism-independent roles for *ADCY5*. In contrast, calcium rises were unaffected in *ADCY5*-depleted islets exposed to GLP-1. Alterations in  $\beta$ -cell *ADCY5* expression and impaired glucose signaling thus provide a likely route through which *ADCY5* gene polymorphisms influence fasting glucose levels and T2D risk, while exerting more minor effects on incretin action.**

Type 2 diabetes (T2D) is one of the foremost health challenges currently facing developed societies. This metabolic disease, which affects  $\sim 8.3\%$  of the adult

population worldwide (1), usually reflects a failure of the  $\beta$ -cell mass to adapt output to increased peripheral insulin resistance. The resulting hyperglycemia and dyslipidemia lead to debilitating complications, ranging from kidney failure and blindness to cardiovascular disease and cancer (2). Although the maintenance of an adequate functional  $\beta$ -cell mass is critical for avoiding the development of diabetes (3), the molecular basis of  $\beta$ -cell failure is still poorly understood (4).

The mechanisms underlying glucose-stimulated insulin secretion from single  $\beta$ -cells involve uptake of the sugar via specific glucose transporters (5), enhanced ATP synthesis (6), and closure of ATP-sensitive  $K^+$  ( $K_{ATP}$ ) channels (7). The consequent plasma membrane depolarization leads to  $Ca^{2+}$  influx (8) and exocytosis from secretory granules (9), both of which are further potentiated by “ $K_{ATP}$ -independent” amplifying signals (10). In addition, incretin hormones such as glucagon-like peptide 1 (GLP-1) and glucose-dependent insulinotropic peptide, released in response to food transit through the gut, potentiate insulin secretion in a glucose-dependent manner (11). Cognate receptor activation engages adenylate cyclases (ADCYs), enzymes that catalyze the generation of cAMP, a key intra- and intercellular signaling effector in the  $\beta$ -cell. Through its downstream interactions with protein kinase A and exchange protein activated by cAMP (Epac), cAMP drives changes including  $Ca^{2+}$  influx, intracellular  $Ca^{2+}$  mobilization (12), and the enhanced fusion competence of

<sup>1</sup>Section of Cell Biology, Division of Diabetes, Endocrinology and Metabolism, Department of Medicine, Imperial College London, London, U.K.

<sup>2</sup>Department of Endocrinology and Metabolism, University of Pisa, Pisa, Italy

<sup>3</sup>Department of Pharmacology, University of Cambridge, Cambridge, U.K.

<sup>4</sup>Cell Isolation and Transplantation Center, Department of Surgery, Geneva University Hospitals and University of Geneva, Geneva, Switzerland

<sup>5</sup>Diabetes Research Institute, San Raffaele Scientific Institute, Milan, Italy

<sup>6</sup>Nuffield Department of Surgical Sciences, University of Oxford, Oxford, U.K.

<sup>7</sup>Oxford Centre for Diabetes, Endocrinology, and Metabolism, University of Oxford, Oxford, U.K.

<sup>8</sup>National Institute of Health Research Oxford Biomedical Research Centre, Churchill Hospital, Oxford, U.K.

<sup>9</sup>University of Texas Southwestern Medical Center, Dallas, TX

<sup>10</sup>Clinical Islet Laboratory and Clinical Islet Transplant Program, University of Alberta, Edmonton, Alberta, Canada

Corresponding author: David J. Hodson, d.hodson@imperial.ac.uk, or Guy A. Rutter, g.rutter@imperial.ac.uk.

Received 18 October 2013 and accepted 10 April 2014.

This article contains Supplementary Data online at <http://diabetes.diabetesjournals.org/lookup/suppl/doi:10.2337/db13-1607/-/DC1>.

D.J.H. and R.K.M. made equal contributions to this study.

© 2014 by the American Diabetes Association. Readers may use this article as long as the work is properly cited, the use is educational and not for profit, and the work is not altered.

secretory granules (13). By contrast, glucose evokes more modest increases in intracellular cAMP (14), possibly via the stimulation of  $\text{Ca}^{2+}$ -activated ADCYs such as ADCY1 and ADCY10 (15).

Both genetic (16) and environmental (4) risk factors conspire to determine the rate and extent of loss of insulin secretory capacity in T2D. Thus, the majority of genetic risk loci (~70) currently identified by genome-wide association (GWAS) or familial studies alter functional  $\beta$ -cell mass while exerting little, or occasionally a beneficial, effect on insulin sensitivity (17). Of note, recent genetic studies have provided evidence that several pathways converging on  $\beta$ -cell cAMP signaling may influence T2D risk. For example, carriers of the major A-allele at rs11708067, or the C-allele at the neighboring single nucleotide polymorphism (SNP) rs2877716, lying on chromosome 3 in intron 3 of the *ADCY5* gene, have an increased odds ratio of developing T2D (18). *ADCY5* is a  $\text{Ca}^{2+}$ -inhibited type III adenylyate cyclase (19,20), and risk allele carriers present with elevated fasting glucose (21) but not impaired insulinogenic index or area under the curve ( $\text{AUC}_{\text{insulin/glucose}}$  2-h postoral glucose load (22–25). These data strongly imply that *ADCY5* activity may be required for normal insulin release in response to glucose but not incretin, the latter largely accounting for the effects of oral glucose (26). Whether and how SNPs exert control over  $\beta$ -cell function by influencing *ADCY5* expression remain, nonetheless, unclear.

Therefore, the aims of the current study were to 1) establish a link between genotype and *ADCY5* mRNA levels, 2) silence *ADCY5* expression in human islets using specific short hairpin (sh)RNAs, and 3) use in situ imaging approaches and hormone release assays to establish the role of the cyclase in regulating  $\beta$ -cell responsiveness to glucose and incretin.

## RESEARCH DESIGN AND METHODS

### Human Islet Isolation

Human islets were isolated from deceased heart-beating donors at transplantation facilities in Oxford, Geneva, Pisa, Edmonton, and Milan, with the relevant national and local ethics permissions, including consent from next of kin where required, and cultured as described (27). All studies involving human tissue were approved by the National Research Ethics Committee (NRES) London (Fulham), Research Ethics Committee no. 07/H0711/114.

### Mouse Islet Isolation

Male and female C57BL/6 mice, 8–12 weeks of age, were killed by cervical dislocation and pancreatic islets isolated by collagenase digestion as previously described (28). Animal procedures were approved by the home office according to the Animals (Scientific Procedures) Act 1986 of the United Kingdom (PPL 70/7349).

### ADCY5 Genotyping

DNA samples were genotyped for the SNP rs11708067 by restriction fragment length polymorphism analysis, as

the G allele generated an *HhaI* site. A 250-bp region flanking the locus was amplified by PCR using Phire polymerase (Thermo) with the following primers: TCCGGAAGGCAAA CACAGCA and AGCCAGGCTGCACCCAAGTG. The products were digested with *HhaI* and resolved by agarose gel electrophoresis.

### Lentiviral Delivery of shRNA

Lentiviral particles carrying shRNA expression constructs against human *ADCY5* were acquired from Sigma-Aldrich (Supplementary Table 1). Multiplicity of infection was calculated using Turbo-GFP particles on the same backbone (TRC 1.5; Sigma-Aldrich). Specificity of *ADCY5* gene silencing was confirmed in both dissociated and intact islets, assuming 1,000–2,000 cells/islet for the latter. In all cases, lentiviral particles containing scrambled shRNA were used as controls (Con) and islets infected for 48–72 h.

### Generation of Adenoviral Epac2-camps

cDNA encoding the cAMP sensor citrine/cerulean-Epac2-camps (29) was cloned into pShuttleCMV via *HindIII* and *XhoI* sites before recombination with pAdEasy1 and virus production as described (6,30).

### Real-Time PCR

Relative mRNA abundance was quantified by quantitative RT-PCR (qRT-PCR) using SYBR green (31). Primers (Supplementary Table 2) were designed using PerlPrimer (32), specificity validated using a dissociation curve, and amplification efficiency was determined using a dilution series. Expression of each gene was normalized to cyclophilin A (*Ppia*) and *N*-fold change in mRNA expression versus Con calculated using the  $2^{-\Delta\Delta\text{Ct}}$ .

*ADCY5* mRNA levels were measured for expression quantitative trait locus analysis by qRT-PCR of RNA from isolated human islets as described earlier (33). The expression level of *ADCY5* relative to TATA box-binding protein (*TBP*) was determined by qRT-PCR using Taqman primers and reagents (Supplementary Table 3) and the comparative Ct method ( $2^{-\Delta\Delta\text{Ct}}$ ) used for subsequent calculations.

### Immunohistochemistry

Islets were fixed overnight at 4°C in paraformaldehyde before application of primary antibodies against *ADCY5*/6 (cat. no. ab66037; Abcam) (34) and either guinea pig anti-insulin 1:200 or mouse anti-glucagon 1:1,000 (both DAKO). Revelation was performed with goat anti-rabbit Alexa-Fluor 488 and either goat anti-guinea pig Alexa-Fluor 568 or goat anti-mouse Alexa-Fluor 568 antibodies (both 1:500, Invitrogen). Images were acquired as previously described (27).

### Measurements of Insulin Secretion From Isolated Islets

Insulin secretion was measured from groups of five to six islets per well, incubated for 30 min in 0.5 mL Krebs-HEPES-bicarbonate (KHB) solution (130 mmol/L NaCl, 3.6 mmol/L KCl, 1.5 mmol/L  $\text{CaCl}_2$ , 0.5 mmol/L  $\text{MgSO}_4$ ,

0.5 mmol/L  $\text{NaH}_2\text{PO}_4$ , 2 mmol/L  $\text{NaHCO}_3$ , 10 mmol/L HEPES, and 0.1% [w/v] BSA, pH 7.4) at 37°C containing the indicated glucose and GLP-1 (7-36 human amide fragment) (Cambridge Bioscience) concentrations (35). Total islet proinsulin and insulin were measured after acid ethanol extraction and sonication using specific radioimmunoassays (EMD Millipore).

#### Live:dead and TUNEL Assays

Islets were incubated with 3  $\mu\text{mol/L}$  calcein-AM (Life Technologies) and 2.5  $\mu\text{mol/L}$  propidium iodide (Sigma-Aldrich) before detection of absorbance/emission at 491/525 nm and 561/620 nm, respectively. The islet area occupied by dead cells was expressed as a unitary ratio versus that occupied by live cells. Apoptosis was assessed using a TUNEL staining kit (Promega) according to the manufacturer's instructions, and islets were counterstained against insulin before detection of absorbance/emission at 491/525 nm and 561/620 nm, respectively.

#### Calcium, ATP/ADP, and cAMP Imaging

Isolated islets were incubated (37°C, 95%  $\text{O}_2$ /5%  $\text{CO}_2$ ) for 1 h in fluo2-AM (10  $\mu\text{mol/L}$ ) diluted in a bicarbonate buffer solution (120 mmol/L NaCl, 4.8 mmol/L KCl, 1.25 mmol/L  $\text{NaH}_2\text{PO}_4$ , 24 mmol/L  $\text{NaHCO}_3$ , 2.5 mmol/L  $\text{CaCl}_2$ , 1.2 mmol/L  $\text{MgCl}_2$ , and 3 mmol/L D-glucose; all Sigma-Aldrich). Functional multicellular  $\text{Ca}^{2+}$  imaging was performed using a Nipkow spinning-disk head and the resulting traces were normalized to minimum fluorescence ( $F_{\text{min}}$ ) (27). A near-identical distribution of Fluo-2 intensity was detected in Con and ADCY5 shRNA-treated islets under resting (3 mmol/L glucose) conditions, indicating that basal  $\text{Ca}^{2+}$  levels were likely unaffected by gene knockdown, assuming similar dye loading (Supplementary Fig. 1).

For imaging of cytosolic ATP/ADP with Perceval (6) or cAMP with Epac2-camps, islets were infected for 48 h with adenoviruses at multiplicity of infection 10–100, giving infection of the first 2–3 islet cell layers. Cells were imaged using a HEPES-bicarbonate buffer (120 mmol/L NaCl, 4.8 mmol/L KCl, 24 mmol/L  $\text{NaHCO}_3$ , 0.5 mmol/L  $\text{Na}_2\text{HPO}_4$ , 5 mmol/L HEPES, 2.5 mmol/L  $\text{CaCl}_2$ , and 1.2 mmol/L  $\text{MgCl}_2$ ). For Perceval, absorbance/emission was 491/525 nm. For the Epac2-camps probe, excitation was delivered at 440 nm and emitted signals captured using cerulean (530 nm) and citrine (470 nm) filters. Förster resonance energy transfer (FRET) was calculated as the ratio of cerulean:citrine fluorescence and, for each experiment, expressed as a percentage of that obtained after maximal stimulation with 50  $\mu\text{mol/L}$  forskolin (FSK). No differences in probe responses to FSK were detected in Con and ADCY5 shRNA-treated tissue ( $F/F_{\text{min}} = 1.07 \pm 0.01$  vs.  $1.06 \pm 0.01$  arbitrary units [AU], Con vs. ADCY5, respectively;  $P > 0.05$ ).

#### ZIMIR Imaging

ZIMIR, a membrane-bound probe that fluoresces upon binding of zinc ( $\text{Zn}^{2+}$ ) coreleased with insulin from granules, was used to dynamically monitor insulin secretion as

previously described (27,36). Briefly, islets were incubated with 10  $\mu\text{mol/L}$  ZIMIR for 2 h and imaged in bicarbonate buffer supplemented with 1  $\mu\text{mol/L}$  EGTA. After acquisition (absorbance/emission = 491/525 nm), islets were divided into 20 subregions before extraction of intensity over time traces and analysis of amplitude and AUC.

#### Total Internal Reflection of Fluorescence Microscopy

Insulin-stained PFA-fixed islets were subjected to total internal reflection of fluorescence imaging to capture a superresolution snapshot of submembrane insulin granule distribution. The evanescent field was produced using a 561-nm laser (CrystaLaser) and a 100 $\times$  1.6 NA objective (Zeiss). Insulin granule density was expressed as a unitary ratio versus the total membrane area, the latter being clearly visible between adjacent cells.

#### Correlation and Frequency Analysis

Correlation and frequency analyses were performed as previously detailed (27,37). Briefly, intensity over time traces were extracted for each fluo-2-loaded cell using a region of interest before manual triage for glucose responsiveness based on rises above a 25% threshold. The Pearson product moment correlation was performed for all possible cell pair combinations and significance ( $P < 0.05$ ) calculated versus the expected  $t$  distribution of independent  $R$  values. Functional connectivity maps showing the location of significantly correlated cell pairs were then constructed based upon correlation strength and position within the imaged field ( $x$ - $y$ ). Phase maps were compiled by converting the normalized intensity of each cell to a value between 1 and 100% and assigning this to a color using a light-dark ramp.  $\text{Ca}^{2+}$ -spiking frequency was measured using the fast Fourier transform.

#### Statistical Analysis

Data distribution was determined using D'Agostino omnibus or Shapiro-Wilk tests. Nonmultifactorial pairwise comparisons were made using Mann-Whitney  $U$  test or Student unpaired and paired  $t$  tests. Two-way ANOVA was used to assess interactions between multiple treatments ( $P < 0.01$ ), and pairwise comparisons were performed using Bonferroni posttests. Expression quantitative trait locus data were stratified according to genotype, BMI, age, and sex. Factors included in the model were selected using the Akaike Information Criterion, resulting in the exclusion of age and BMI, as these were uninformative with regard to ADCY5 expression. To account for any prediction error, linear regression analyses were performed separately for both excluded variables, yielding nonsignificant relationships ( $P > 0.05$ ). Owing to a significant interaction between sex and genotype in donors 22–70 years of age ( $P = 0.0476$ ; two-way ANOVA), effects of genotype on mRNA abundance were assessed within sex group using one-way ANOVA. In all cases, analysis was performed using R (R Project), GraphPad Prism (GraphPad Software), IgorPro (Wavemetrics), and MATLAB (Mathworks), and results were considered significant at  $P < 0.05$ .

## RESULTS

### ADCY5 Is Expressed in Human Islets at the mRNA and Protein Level

We sought firstly to characterize ADCY5 expression in tissue isolated from human and murine donors. Confirming previously published microarray data (33), SYBR Green qRT-PCR analyses revealed that *ADCY5* and *ADCY6* transcript levels were similar in human but not mouse islets (Fig. 1A). Immunohistochemistry using an antibody against ADCY5, and with some reported cross-reactivity against ADCY6, demonstrated the localization of both enzymes in the cytoplasm of insulin and glucagon immunopositive cells throughout individual human islets (Fig. 1B).

### ADCY5 mRNA Levels Are Influenced by Genotype

While GWAS provides statistically powerful information concerning associations between SNPs and T2D risk, it is unable to report on how the expression of genes at variant *loci* is altered in tissues implicated in glucose homeostasis. Since the elevated glucose levels associated with T2D may influence *ADCY5* expression, we attempted to correlate genotype at SNP rs11708067 with *ADCY5* mRNA abundance using tissue from a catalog of healthy donors. Allele frequency was close to that expected from previous studies (~75% A) (18), and Taqman qRT-PCR analysis of RNA from isolated islets revealed approximately twofold lower mean *ADCY5* expression in male AA versus AG carriers <70 years of age (Fig. 1C and Supplementary Table 4). When considered separately, neither age nor BMI significantly influenced *ADCY5* expression for either genotype (Fig. 1D and E).

### ADCY5 Is Required for Glucose-Stimulated Insulin Secretion

Given the above association between *ADCY5* expression and fasting glucose levels and genotype in man, we next explored a role for this gene in human  $\beta$ -cell stimulus-secretion coupling. shRNAs directed against various sequences of the *ADCY5* gene were delivered into dispersed cells or islets using replication-incompetent lentiviruses ( $n = 26$  separate normoglycemic donors) (see Supplementary Table 5). Gene silencing efficiency was determined using qRT-PCR (Fig. 2A and B), and effects were confirmed at the protein level using immunohistochemistry and an antiserum raised against ADCY5/6 (Fig. 2C). Although mRNA levels were less affected by shRNA in intact than dissociated islets, this was most likely due to limited penetration of virus into the islet core (38); cells within the imaged layers were nevertheless typified by the near-complete absence of ADCY5 immunoreactivity. *ADCY6* mRNA abundance was not altered by *ADCY5* silencing, suggesting that the action of the shRNA on immunoreactivity was largely due to loss of the latter mRNA message (Fig. 2D). Cell viability and apoptosis indices were normal, excluding any effects of impaired cAMP signaling on  $\beta$ -cell survival (Fig. 2E and F).

The impact of *ADCY5* silencing on glucose- or incretin-stimulated insulin secretory dynamics was subsequently

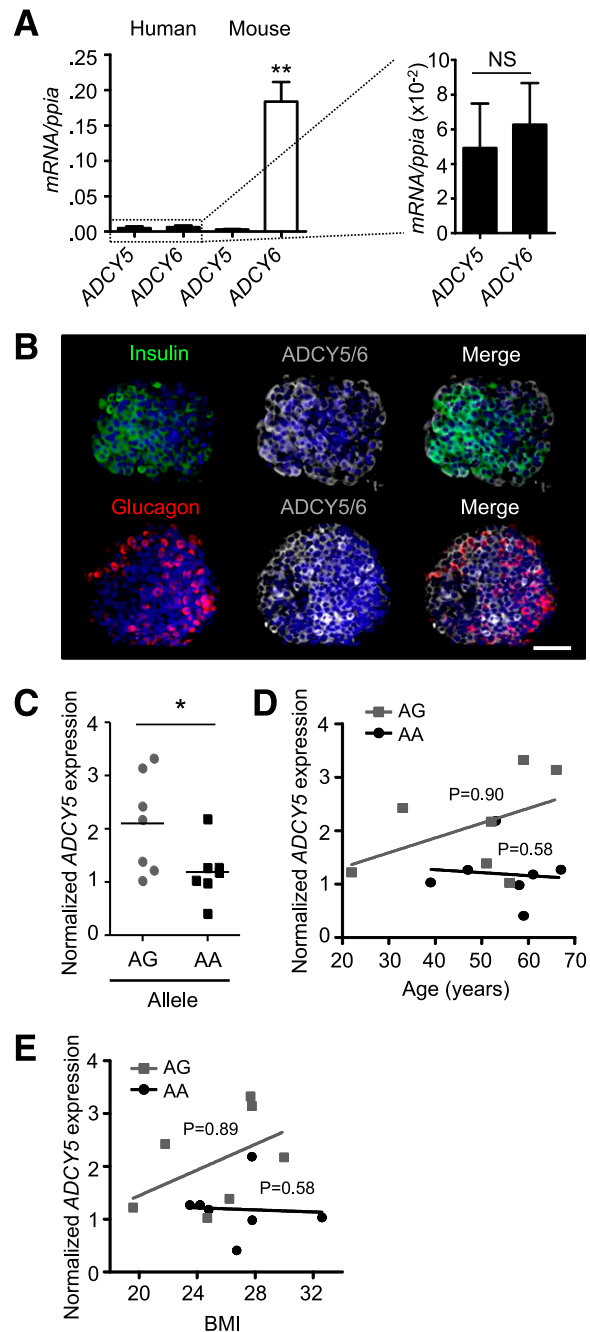


**Figure 1**—ADCY5 is expressed in isolated human islets and affected by T2D risk alleles. **A**: *ADCY5* and *ADCY6* are expressed at similar levels in human islets ( $n = 4$  donors). Conversely, *Adcy6* mRNA expression is ~40-fold more abundant than that of *Adcy5*, which is barely detectable in mouse islets ( $n = 3$  female and 3 male animals;  $**P < 0.01$  vs. *ADCY5*, Student  $t$  test). **B**: Immunostaining using an anti-ADCY5 immunoglobulin, with some reported cross-reactivity to ADCY6, reveals the cytoplasmic distribution of both proteins throughout the human  $\alpha$ - and  $\beta$ -cell populations (DAPI, blue; scale bar, 60  $\mu$ m). **C**: Scatter plot showing reduced *ADCY5* mRNA abundance in islets from males <70 years of age who are carriers of the AA risk allele at rs11708067 ( $*P < 0.043$  vs. AG; one-way ANOVA;  $n = 7$  donors for each allele). Values represent mean  $\pm$  SEM. **D**: Age of donors is not significantly correlated with *ADCY5* mRNA expression ( $R^2 = 0.21$  and  $R^2 = 0.01$  for AG and AA, respectively; linear regression) ( $P$  values shown on graph). **E**: As for **D**, but BMI ( $R^2 = 0.23$  and  $R^2 = 0.003$ , AG vs. AA, respectively; linear regression) ( $P$  values shown on graph).

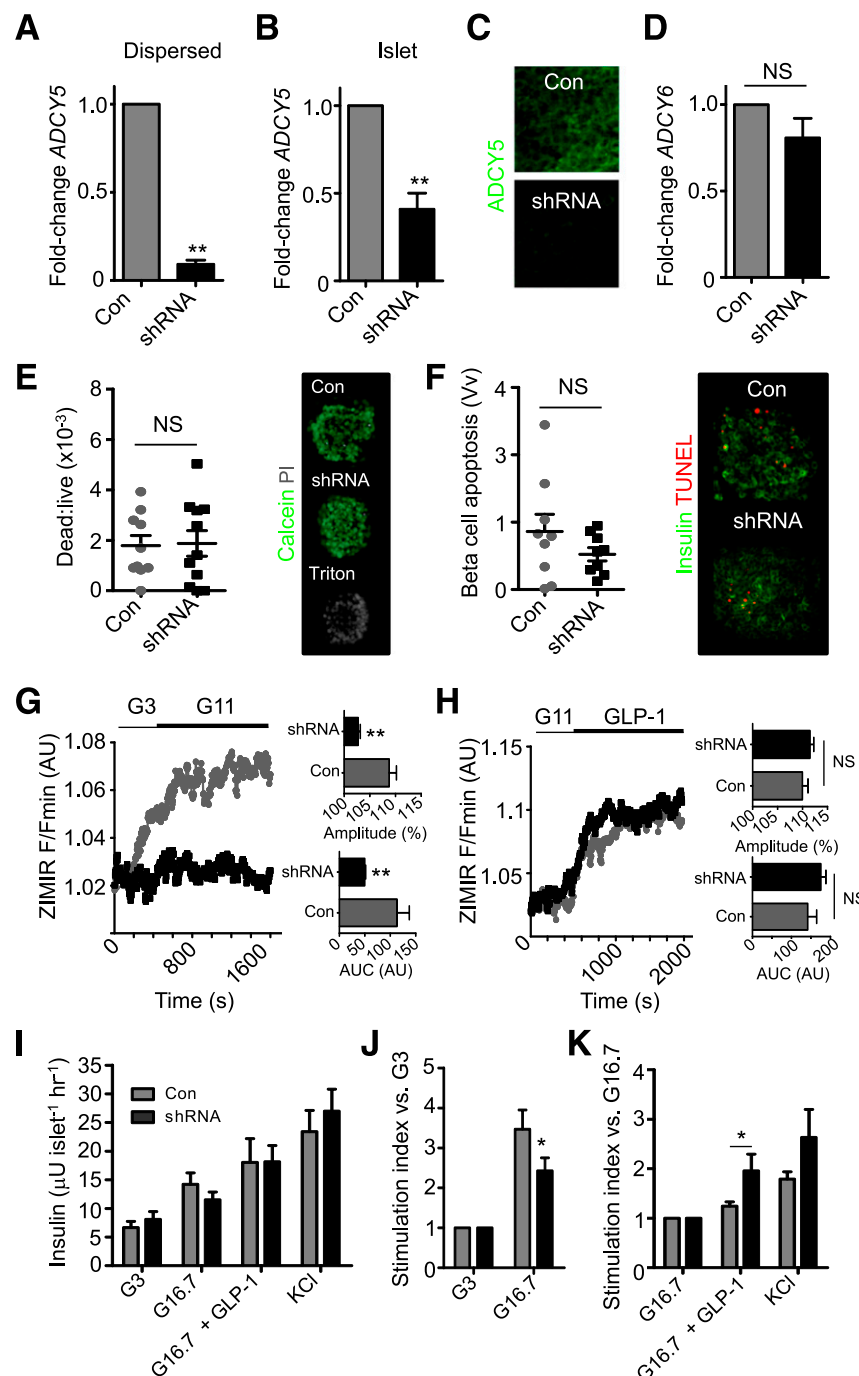


**Figure 2**—ADCY5 silencing inhibits glucose- but not GLP-1-stimulated insulin secretion. **A** and **B**: Lentivirus harboring shRNA against ADCY5 reduces expression by >50% in both dispersed and intact islets (\*\**P* < 0.01 vs. Con; Student paired *t* test; *n* = 3–4 donors). **C**: ADCY5/6 protein expression is markedly reduced in the first few cell layers of intact islets, as determined using confocal imaging (*n* = 6 islets from two donors). **D**: ADCY6 mRNA expression is unaffected by ADCY5 silencing (NS, nonsignificant vs. Con; Student paired *t* test; *n* = 4 donors). **E**: Dead:live cell ratio is similar in Con and shRNA-treated islets (positive Con, Triton X-100; NS, nonsignificant vs.; Mann-Whitney *U* test; *n* = 10–11 islets from three donors). **F**: As for **E**, but TUNEL assay for apoptosis (*n* = 9 islets from three donors). The proportion of apoptotic β-cells was expressed as a fraction area versus nonapoptotic insulin-positive cell mass (Vv). **G**: ADCY5 knockdown suppresses glucose-induced insulin secretory dynamics, as shown by bar graphs of AUC and amplitude of ZIMIR responses (mean traces, *left panel*; *n* = 8–9 islets from four donors) (\*\**P* < 0.01 vs. Con; Mann-Whitney *U* test). **H**: GLP-1-stimulated insulin secretory dynamics are subtly improved after ADCY5 depletion (mean traces, *left panel*; AUC and amplitude, *right panel*; *n* = 7 islets from three donors) (NS, nonsignificant). **I**: Glucose-stimulated insulin release into static culture is impaired in shRNA-treated islets, as determined using radioimmunoassay (G3 and G16.7, 3 mmol/L and 16.7 mmol/L glucose, respectively) (*n* = 4–8 donors). KCl 30 mmol/L was added as a Con. **J**: As for **I**, but stimulation index vs. 3 mmol/L glucose to better account for the variation between islet preparations (\**P* < 0.02 vs. Con at 16.7 mmol/L glucose; Mann-Whitney *U* test). **K**: As for **J**, but vs. 16.7 mmol/L glucose (G16.7) (\**P* < 0.01 vs. 16.7 mmol/L glucose for each group; Mann-Whitney *U* test). Values represent mean ± SEM. hr, hour.



assessed using Nipkow spinning-disk microscopy (27) to image  $\text{Zn}^{2+}$  coreleased from insulin-containing granules within individual ZIMIR-stained islets (27,36). The amplitude and AUC of glucose (11 mmol/L)-stimulated insulin release were markedly impaired in islets silenced for *ADCY5* (Fig. 2G). By contrast, insulin-release dynamics in response to GLP-1 were subtly improved in tissue depleted for *ADCY5*, suggesting the presence of an intact incretin axis (Fig. 2H). The observations with ZIMIR were confirmed using conventional static incubation techniques followed by radioimmunoassay of supernatant, and we further detected no significant effect of gene silencing on KCl-stimulated insulin release (Fig. 2I–K). Donor variability was largely accounted for by a paired experimental design, and this was further supported by linear regression analyses, which revealed no relationship between age, BMI, and the magnitude suppression of glucose-stimulated insulin release in *ADCY5*-silenced islets (Supplementary Fig. 2). Insulin content was similar in Con and *ADCY5* shRNA-treated islets, although there was a tendency toward an increased proinsulin-to-insulin ratio in the latter (Table 1), as expected from studies in patients harboring SNPs in or near the *ADCY5* locus (25). Lastly, and in line with the secretory measures, total internal reflection of fluorescence imaging of insulin-stained islets confirmed that *ADCY5* knockdown did not alter the distribution of granules located in the vicinity of the plasma membrane (Supplementary Fig. 3A and B).

#### **ADCY5 Couples Glucose to cAMP Generation, $\text{Ca}^{2+}$ Rises, and $\beta$ -Cell Connectivity**

Using Epac2-camps (29) to measure cAMP rises in  $\beta$ -cells (Supplementary Fig. 4), almost a threefold reduction in glucose- but not FSK-stimulated cAMP generation could be detected in *ADCY5*-silenced islets (Fig. 3A and B). Since cAMP elevations are linked to enhanced electrotonic coupling (39), the effects of *ADCY5* depletion on the cell-cell communication processes underlying the intraislet regulation of insulin secretion were next investigated. Cytosolic free  $\text{Ca}^{2+}$  levels were thus used as a proxy to measure the electrical dynamics known to orchestrate  $\text{Ca}^{2+}$ -dependent hormone secretion from the hundreds of cells residing within the first few microorgan layers; under the conditions used,  $\text{Ca}^{2+}$  changes chiefly reflect those within  $\beta$ -cells (27). In line with its dramatic effects on secretion, *ADCY5* silencing suppressed both the amplitude and AUC of glucose-evoked  $\text{Ca}^{2+}$  rises throughout the imaged population (Fig. 3C–E and Supplementary Movies 1 and 2) ( $n = 3$  donors;

BMI range = 25.4–27.4; age range = 52–76 years). Furthermore, connectivity between individual  $\beta$ -cells, analyzed by large-scale mapping of long-term ( $\sim 30$  min) evolutions in correlated cell-cell interactivity (40) and recently shown to be a key element in the insulin secretory response (27,41), was also reduced in *ADCY5*-silenced islets (Fig. 3F and G). Neither the number of responsive cells (Fig. 3H) nor the frequency of  $[\text{Ca}^{2+}]_i$  oscillations (Fig. 3I) was affected by *ADCY5* knockdown, suggesting that the absence of the cyclase was unlikely to impair insulin release by targeting the rhythmicity of a  $\beta$ -cell subpopulation. Implying that the effects of silencing were unlikely to reflect a long-term consequence of *ADCY5* depletion, a similar degree of suppression of glucose-induced  $\text{Ca}^{2+}$  rises was obtained using 20  $\mu\text{mol/L}$  NKY80, a relatively selective chemical inhibitor of the enzyme ( $\text{IC}_{50} = 8.3 \mu\text{mol/L}$ , 132  $\mu\text{mol/L}$ , and 1.7 mmol/L for *ADCY5*, 3, and 2, respectively) (42) (Supplementary Fig. 5A). Demonstrating the specificity of both shRNA and NKY80, the inhibitory actions of the drug were lost after *ADCY5* silencing (Supplementary Fig. 5B).

#### **GLP-1-Stimulated $\beta$ -Cell Activity Does Not Involve *ADCY5***

Consistent with the lack of effect of gene silencing on GLP-1-induced insulin release, loss of *ADCY5* failed to impact  $\text{Ca}^{2+}$  changes and even appeared to augment  $\text{Ca}^{2+}$  increases in response to the incretin without modulating the proportion of responsive cells (Fig. 4A and B and Supplementary Movies 3 and 4). Furthermore, GLP-1-mediated increases in  $\beta$ -cell- $\beta$ -cell connectivity, critical for generating the acute (5–10 min) bursts in coordinated activity that underlie incretin potentiation of glucose-stimulated insulin secretion (27), were unchanged after treatment with anti-*ADCY5* shRNA (Fig. 4C–E). In line with this, *GLP-1R* mRNA expression levels were unaffected by *ADCY5* silencing (Fig. 4F).

#### **Glucose Still Increases Cytosolic ATP-to-ADP Ratio After *ADCY5* Silencing**

We wondered whether the substantial reductions in glucose-induced  $\text{Ca}^{2+}$  rises and insulin release, detected in *ADCY5*-silenced islets, were accompanied by fulminant changes to  $\beta$ -cell glucose metabolism. To allow the real time recording of ATP dynamics specifically in  $\beta$ -cells, the expression of the recombinant probe Perceval was directed in human islets using an adenoviral vector (6,43). Confirming tropism of the virus for  $\beta$ -cells, as previously described in rodent islets (44), green fluorescent protein fluorescence was restricted to insulin-immunopositive cells (Fig. 5A). In response to increasing glucose concentrations (3–17 mmol/L),  $\beta$ -cells responded with large, coordinated, and nonoscillatory elevations in ATP-to-ADP ratio (Fig. 5B). Although significantly reduced, a glucose-induced increase in ATP-to-ADP ratio could still be detected after *ADCY5* silencing (Fig. 5C). Further excluding a role for cAMP-independent effects on  $K_{\text{ATP}}$  or voltage-dependent  $\text{Ca}^{2+}$  channel (VDCC) activity, *ADCY5* silencing

**Table 1—Insulin and proinsulin content in Con and *ADCY5* shRNA-treated islets ( $n = 4$  donors)**

	Con	shRNA
Proinsulin content (ng/islet)	$0.82 \pm 0.11$	$0.93 \pm 0.07$
Insulin content (ng/islet)	$32.8 \pm 3.5$	$29.8 \pm 3.1$
Proinsulin:insulin (%)	$2.6 \pm 0.5$	$4.0 \pm 1.2$

Data are means  $\pm$  SEM.

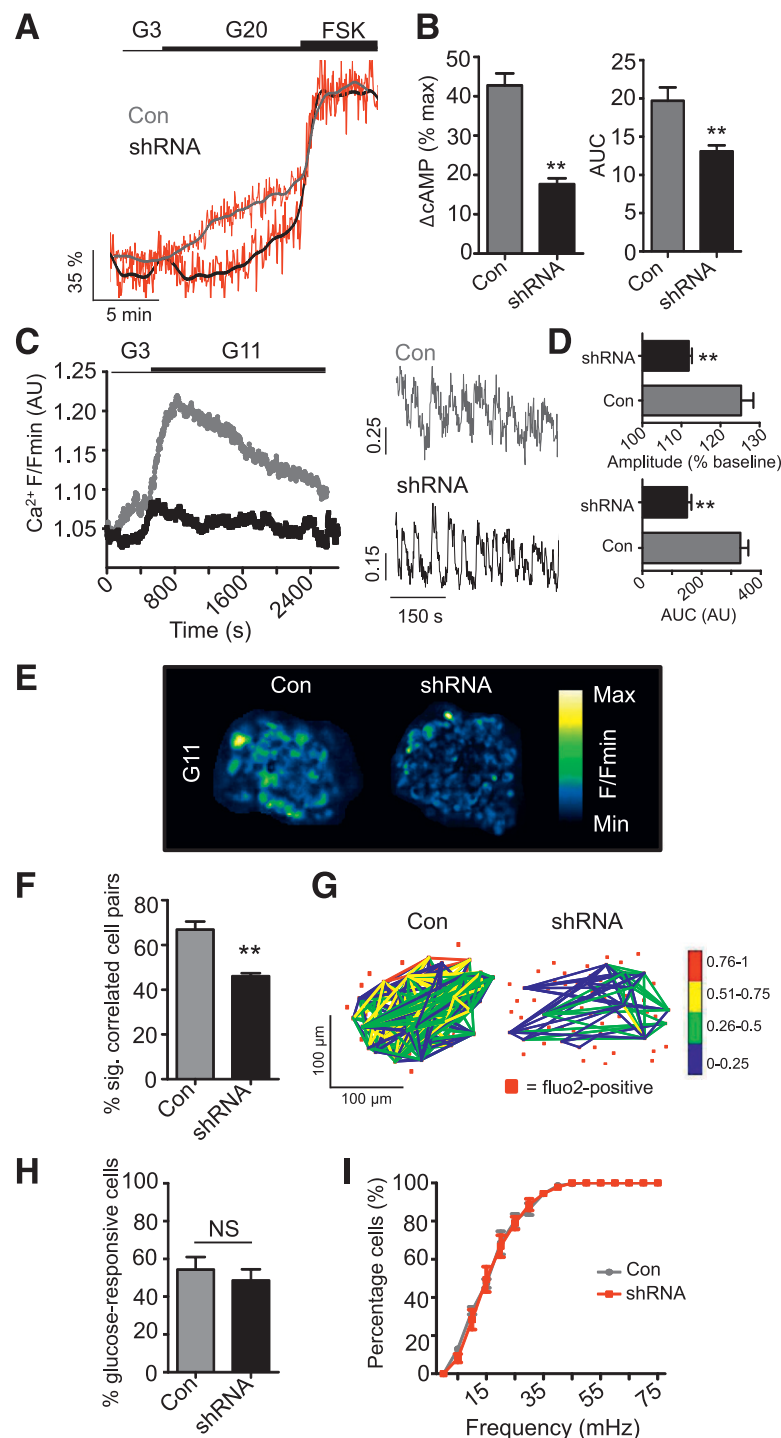


**Figure 3**—ADCY5 depletion suppresses glucose-induced increases in cytosolic free  $\text{Ca}^{2+}$ . **A**: ADCY5 silencing decreases cytosolic cAMP levels, as determined using the recombinant probe Epac2-camps (representative traces shown; gray/black, smoothed; red, raw). **B**: As for **A**, but summary data showing a reduction in measured FRET signal versus maximal stimulation with FSK (%), as well as decreased AUC ( $**P < 0.01$  vs. Con; Student *t* test;  $n = 12$  recordings from three donors). **C**: ADCY5 knockdown suppresses 11 mmol/L glucose (G11)-evoked cytosolic  $\text{Ca}^{2+}$  rises (left panel: mean traces) (right panel: zoom-in of  $\text{Ca}^{2+}$  oscillations). **D**: AUC and amplitude of  $\text{Ca}^{2+}$  rises are reduced in shRNA-treated islets (right panel,  $**P < 0.01$  vs. Con; Mann-Whitney *U* test;  $n = 10$  islets from three donors). **E**: Pseudocolored Con and shRNA-treated human islets during exposure to 11 mmol/L glucose (recording time = 40 min; image cropped to display a single islet). **F**: ADCY5 is required for long-term evolutions in coordinated cell activity after exposure to elevated glucose ( $**P < 0.01$  vs. Con; Mann-Whitney *U* test;  $n = 9$ –10 islets from three donors) (correlation calculated over 20–30 min; sig, significantly). **G**: Representative functional connectivity map depicting location, number, and strength (color-coded; 0 [blue] = lowest, 1 [red] = highest) of significantly correlated cell pairs (Pearson *R* coefficient,  $P < 0.05$ ). Note that ADCY5 silencing decreases both the number and strength of correlations. **H**: Gene silencing does not significantly alter the percentage (%) of glucose (11 mmol/L)-responsive cells (NS, nonsignificant vs. Con; Mann-Whitney *U* test). **I**: The cumulative distribution of  $\text{Ca}^{2+}$ -spiking frequencies remains similar in Con and shRNA-treated islets. Values represent mean  $\pm$  SEM.



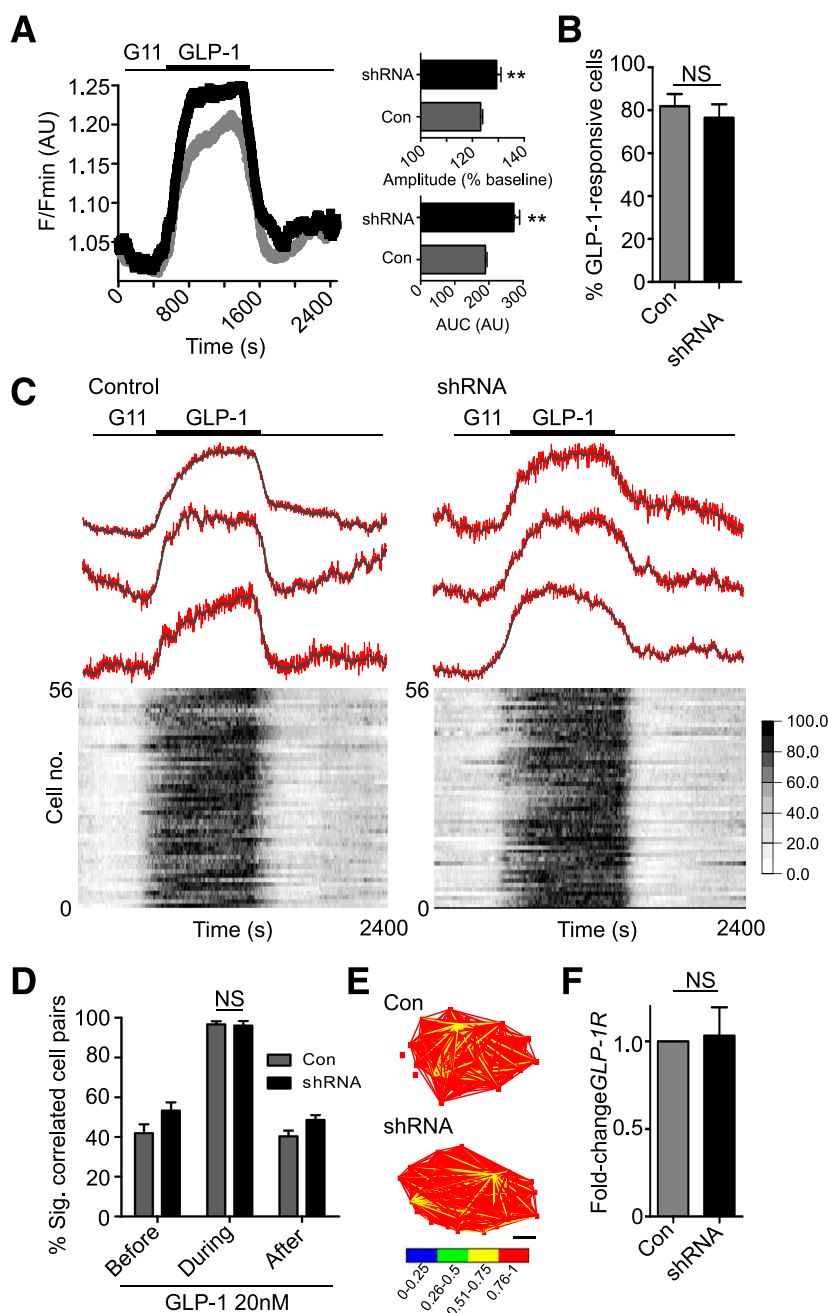


**Figure 4**—ADCY5 does not mediate GLP-1-stimulated cytosolic  $\text{Ca}^{2+}$  increases. **A**: ADCY5 knockdown subtly improves GLP-1 responses (*left panel*: mean traces), as evidenced by increased AUC and amplitude of cytosolic  $\text{Ca}^{2+}$  rises in shRNA-treated islets (*right panel*) (\*\* $P < 0.01$  vs. Con; Mann-Whitney  $U$  test;  $n = 10$  islets from three donors). **B**: The proportion of GLP-1-responsive cells is similar in Con and shRNA-treated islets (NS, nonsignificant vs. Con; Mann-Whitney  $U$  test). **C**: ADCY5 silencing does not affect coordinated  $\beta$ -cell responses to 11 mmol/L glucose plus GLP-1 (representative  $\text{Ca}^{2+}$  traces [*top panel*]; gray, smoothed; red, raw) (heat map depicting minimum–maximum for each cell [*bottom panel*] ( $n = 10$  islets from three donors; correlation measured using 5-min windows)). **D**: Histogram showing mean % significantly correlated cell pairs in Con and shRNA-treated islets before, during, and after GLP-1 application (NS, nonsignificant; two-way ANOVA). **E**: Representative weighted graphs demonstrating large increases in  $\beta$ -cell connectivity after exposure to GLP-1 in both normal and ADCY5-depleted islets (scale bar, 50  $\mu\text{m}$ ). **F**: Gene silencing does not alter *GLP-1R* mRNA expression (NS, nonsignificant vs. Con; Student paired  $t$  test;  $n = 3$  donors). Values represent mean  $\pm$  SEM.

did not alter  $\text{Ca}^{2+}$  rises induced by KCl applied in the absence and presence of the  $\text{K}_{\text{ATP}}$  channel opener, diazoxide (Supplementary Fig. 6A and B). Consistent with our previous findings in MIN6  $\beta$ -cells (12), GLP-1 was able to provoke significant rises in ATP-to-ADP ratio under both

low (3 mmol/L) and high (16.7 mmol/L) glucose conditions (Fig. 5D–F), as well as in the presence of ADCY5 silencing (Fig. 5G and H). Hence, an action of glucose to accelerate oxidative metabolism toward ATP synthesis is not a prerequisite for GLP-1 signaling.

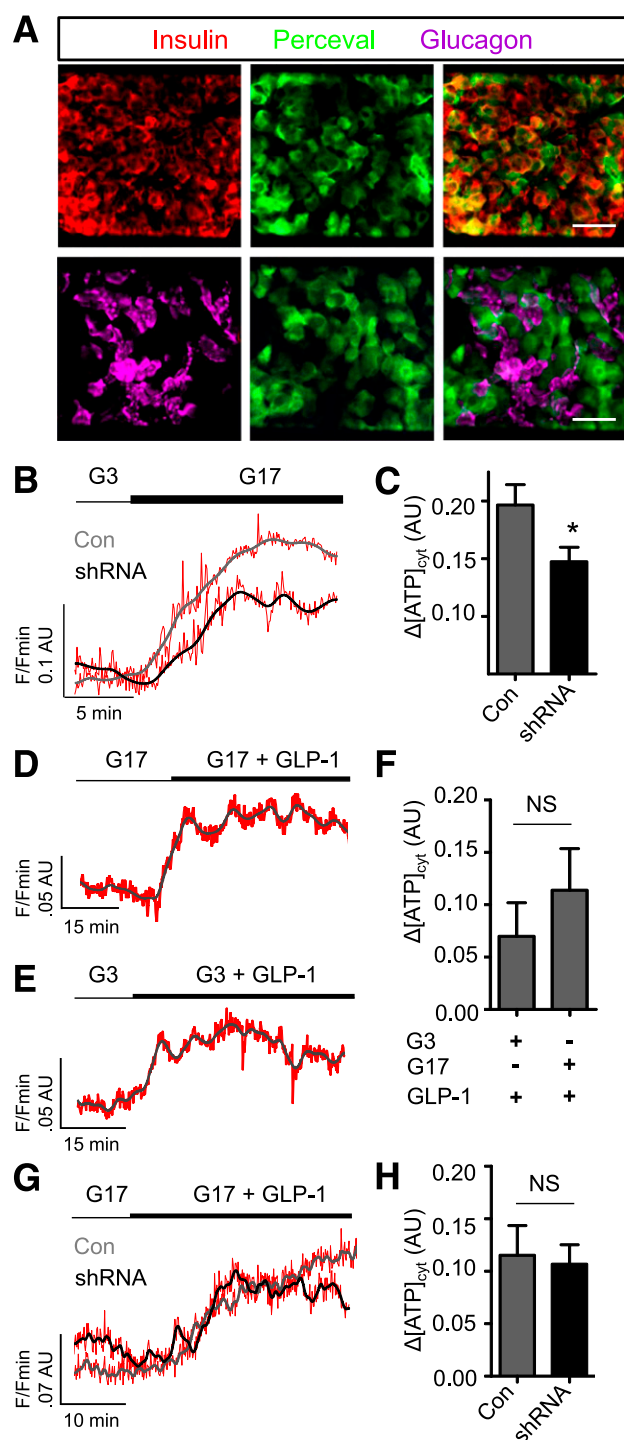


**Figure 5—ADCY5 alters  $\beta$ -cell energetics.** A: Expression of the ATP/ADP probe Perceval is predominantly restricted to  $\beta$ -cells, as shown using immunohistochemistry with antibodies against insulin and glucagon (scale bar, 25  $\mu$ m [top panels] and 20  $\mu$ m [bottom panels]). B: Glucose (17 mmol/L) (G17) still induces increases in ATP-to-ADP ratio after ADCY5 silencing (representative traces shown; gray/black, smoothed; red, raw). C: Bar graph showing a significant effect of shRNA treatment on the amplitude of cytosolic (cyt) ATP/ADP rises in response to 17 mmol/L glucose (\* $P < 0.05$  vs. Con; Mann-Whitney  $U$  test;  $n = 9$ –10 islets from three donors). D: GLP-1 increases ATP/ADP in the presence of permissive (17 mmol/L) glucose concentrations (representative traces shown; gray/black, smoothed; red, raw). E: As for D, but in the presence of nonpermissive (3 mmol/L) glucose concentrations. F: Summary statistics

To determine the relative contribution of metabolism to ADCY5-regulated  $\beta$ -cell function, ATP-to-ADP dynamics were imaged after exposure to increasing glucose concentrations. Whereas both Con and ADCY5-silenced islets responded normally to 5 and 8 mmol/L glucose (Fig. 6A), the latter failed to respond to further elevation of the sugar, and this deficit could be rescued using FSK to elevate cAMP (Fig. 6B). Cytosolic  $Ca^{2+}$  responses to 8 mmol/L glucose, however, remained suppressed after ADCY5 knock-down (Fig. 6C).

## DISCUSSION

The aim of the current study was to explore the role of ADCY5 in the regulation of insulin secretion from human islets. We show that ADCY5 is required to link glucose-derived signals to the intracellular  $Ca^{2+}$  rises that principally drive insulin granule exocytosis. By contrast, incretins such as GLP-1 remain competent to evoke insulin release in the face of ADCY5 silencing (Fig. 7). Providing compelling evidence that defective ADCY5 action may contribute to impaired fasting glucose were the observations that mRNA expression was reduced in islets from subjects harboring risk alleles at rs11708067. Interestingly, ADCY5 mRNA levels were also reduced in  $\beta$ -cells from (ungenotyped) patients with T2D versus healthy donors (33), providing a further link with disease status.

Assessed by next-generation sequencing (RNA-Seq), ADCY5 mRNA occupies the top 13th centile of all mRNAs in human islets (45) and is the most strongly expressed member of the ADCY family in this tissue, with mRNA levels approximately twofold higher than those of ADCY1, the next most abundant isoform, and 50% higher than ADCY6 mRNA. Assuming similar levels of PPIA mRNA, our qRT-PCR results in isolated human islets are broadly consistent with this observation (Fig. 1A). Of note, however, analysis of laser-capture-dissected  $\beta$ -cells (33) (Gene Expression Omnibus public repository, accession no. GSE20966) and a  $\beta$ -cell-enriched fraction from human islets (46) revealed lower levels of ADCY5 mRNA ( $\sim$ 50th and  $\sim$ 65th centiles, respectively), being in each case  $\sim$ 50% of those of ADCY6. Intriguingly, in the current study, *Adcy5* mRNA was barely detectable in mouse islets, being expressed at a level  $\sim$ 40-fold lower than *Adcy6* (Fig. 1). A similar, though less marked (approximately eightfold), preponderance of ADCY6 over ADCY5 mRNA also exists for rat islets (47), demonstrating marked species variability in the relative abundance of

demonstrate similar effects of GLP-1 on ATP/ADP in islets exposed to 3 or 17 mmol/L glucose (NS, nonsignificant vs. Con; Mann-Whitney  $U$  test;  $n = 10$ –13 recordings from five donors). G: ATP/ADP responses to GLP-1 are similar in Con and ADCY5 shRNA-treated islets (representative traces shown; gray/black, smoothed; red, raw). H: Summary statistics demonstrate no significant effect of gene silencing on GLP-1-induced ATP/ADP rises (NS, nonsignificant vs. Con; Mann-Whitney  $U$  test;  $n = 6$  recordings from two donors). Values represent mean  $\pm$  SEM.

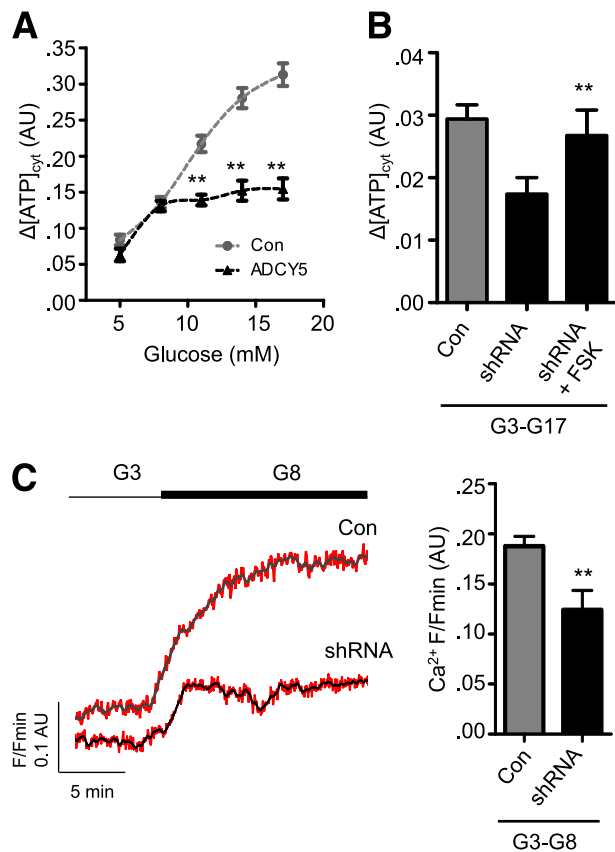


**Figure 6**—ADCY5 targets nonmetabolic processes to alter  $\text{Ca}^{2+}$  responses. **A:** Impaired ATP/ADP responses are only present in ADCY5-silenced islets at glucose concentrations of  $\geq 11$  mmol/L ( $**P < 0.01$  vs. Con; two-way ANOVA;  $n = 9$  recordings from three donors). **B:** Elevation of cAMP using FSK rescues ATP/ADP rises in ADCY5-silenced islets after transition from 3 mmol/L to 17 mmol/L glucose (G3-G17) ( $**P < 0.01$  vs. shRNA; one-way ANOVA;  $n = 9$  recordings from three donors;  $n = 4$ –5 recordings). **C:** ADCY5 knockdown suppresses  $\beta$ -cell  $\text{Ca}^{2+}$  responses after transition from 3 mmol/L to 8 mmol/L glucose (G3-G8) (representative traces [left panel]; gray/black, smoothed; red, raw), as evidenced by reduced amplitude (right panel) ( $**P < 0.01$  vs. shRNA; Mann-Whitney  $U$  test;  $n = 8$ –9 recordings from three donors).

ADCY isoforms within this tissue. Since these variations do not appear to reflect the greater proportion of  $\alpha$ -cells in human (48) versus rodent (49) islets, ADCY5 may serve a nonconserved function between mammalian species.

Levels of mRNA encoding ADCY8, previously reported to be regulated by glucose in rat and human islets (50), were recently shown to be much lower in human islets than either ADCY5 or -6 (45). Confirming these findings, ADCY8 mRNA was undetectable in four out of the five independent repeats that we conducted in human islets, and in the single experiment in which an amplicon was present,  $C_t$  values were incompatible with accurate quantification ( $37.05 \pm 0.49$  cycles).

Of other genes lying 250 kb on either side of rs2877716 and rs11708067, which might also conceivably mediate the observed effects on diabetes risk, MYLK

transcripts are barely detectable in human islets (45,46). On the other hand, SEC22A, PDIA, and PTPLB are each detectably expressed and so may contribute. Nonetheless, our observations on the effects of ADCY5 silencing are entirely consistent with the observed phenotype of subjects possessing risk alleles (22).

The strong dependence of glucose-stimulated insulin secretion upon ADCY5 expression in human islets is surprising given the abundant presence of ADCY6 and the redundancies inherent to the cAMP signaling cassette (51). Although the above differences at the mRNA level are not necessarily reflective of protein quantity or enzymatic activity, the observed sensitivity to ADCY5 depletion may reflect either microcompartmentalization of ADCY5-containing complexes in proximity to  $\text{Ca}^{2+}$  influx and release sites (52) or a requirement for ADCY5 in cAMP-independent signaling processes. Thus, while our data indicate that ADCY5 couples glucose to insulin secretion by translating a glucose signal into cAMP generation (53), GLP-1 receptors may engage alternative ADCY family members to modify cAMP dynamics. Further studies will be required to explore the latter possibility (Fig. 7). Of note, global deletion of ADCY5 in mice leads to longevity and the resistance of cardiomyocytes to oxidative stress via the upregulation of Ras-MAPK signaling (20). A similar mechanism might therefore contribute to the small but significant enhancement of GLP-1 signaling observed here in human  $\beta$ -cells after ADCY5 silencing.

Although ADCY5 is  $\text{Ca}^{2+}$  inhibited in vitro (19), the range of  $\text{Ca}^{2+}$  concentrations over which inhibition occurs ( $>10 \mu\text{mol/L}$ ) comfortably exceeds normal intracellular concentrations of these ions in  $\beta$ -cells (8). Whether ADCY5 is therefore a direct target for activation by intracellular signals generated by glucose (ATP, etc.) or is, rather, a passive but essential element of a glucose-activated signaling pathway leading to  $\text{Ca}^{2+}$  influx and insulin release remains to be established.

Recent studies have shown that the intraislet regulation of cell-cell communication is critical for the proper generation of hormone release after secretagogue challenge (27). Providing further evidence that the islet context is an important player in insulin secretion was the observation in the current study that  $\beta$ -cell responses to glucose were less coordinated in islets depleted of ADCY5. While the mechanisms underlying this phenomenon remain obscure, cAMP has been shown to alter  $\beta$ -cell gap junction conductance (39), and the resultant enhanced intercellular coupling may contribute to the insulin-raising actions of cAMP-elevating agents such as glucose and incretins. Whereas we recently showed that knockdown of connexin 36 markedly reduced coordinated cell responses to incretin, more modest effects on glucose action were observed (27). The impact of cAMP on glucose-induced cell connectivity may therefore also stem from perturbed paracrine signaling circuits between  $\beta$ -,  $\alpha$ -, and other cell types, in addition to enhanced electrotonic

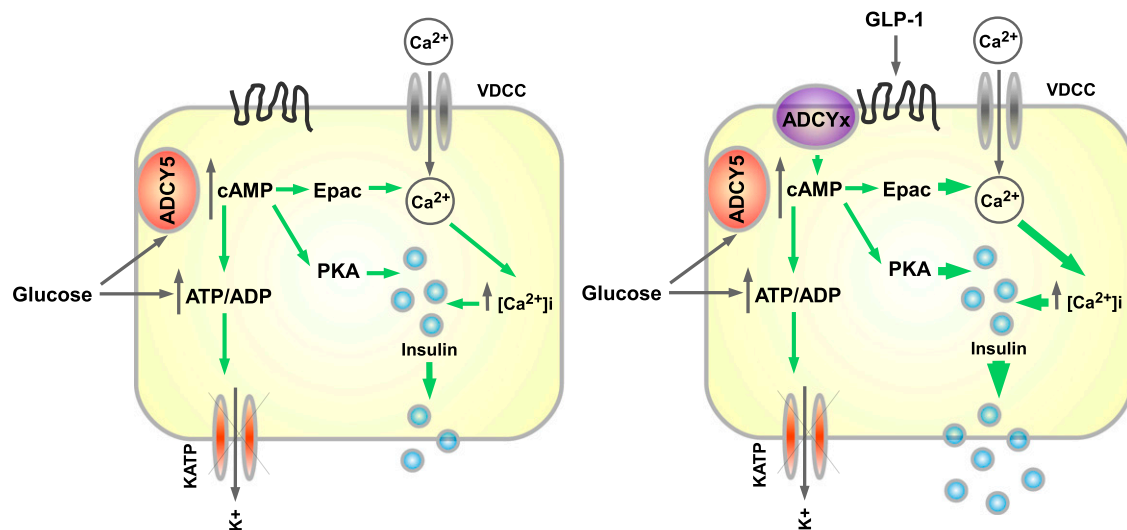


**Figure 7**—Schematic of ADCY5 function in human  $\beta$ -cells. Glucose-stimulated insulin secretion relies on  $K_{ATP}$ -dependent and -independent signals. The latter include cAMP generation, and this likely requires ADCY5 activation by the sugar to increase ATP generation,  $Ca^{2+}$  influx, and exocytosis (*left panel*). By contrast, incretins such as GLP-1, believed primarily to engage cAMP-signaling pathways, may potentiate insulin secretion via other ADCY isoforms (*right panel*). PKA, protein kinase A.

coupling. Likewise, an intriguing possibility is that ADCY5 suppression may also affect glucagon and, potentially, GLP-1 (54) secretion from neighboring  $\alpha$ -cells to affect  $\beta$ -cell “glucose competence.” In any case, ADCY5-depleted islets still displayed impaired  $Ca^{2+}$  responses even when metabolic dysfunction was accounted for (Fig. 6B), supporting the view that other downstream processes, including cell-cell communication, are targeted by cAMP signaling.

Remarkably, GLP-1 evoked  $Ca^{2+}$  rises and hormone release even when glucose-stimulated insulin secretion was abolished by ADCY5 silencing. This implies that GLP-1 signaling—generally believed to hinge on increased intracellular cAMP levels (55)—is sufficient under these conditions to elicit closure of  $K_{ATP}$  and induce  $Ca^{2+}$  influx and exocytosis. Indeed, studies by Miki et al. (56) have demonstrated that GLP-1 is still able to evoke insulin secretion in the complete absence of  $K_{ATP}$  channels. Thus, the glucose dependency of GLP-1-induced insulin secretion is unlikely solely to reflect the effects of the sugar on oxidative metabolism and, hence, the closure of  $K_{ATP}$  channels, especially in light of data showing the absence of GLP-1-induced  $Ca^{2+}$  rises in human islets incubated at nonpermissive glucose concentrations (27). Rather than a simple summation of glucose and GLP-1-derived  $Ca^{2+}$  signals, the ATP/ADP responses to the latter, readily detectable at low glucose concentrations, may instead be converted into a depolarizing stimulus through a complex interplay between  $K_{ATP}$ -dependent and -independent pathways (10).

In summary, we describe here a novel role for the GWAS-identified gene ADCY5 in the normal regulation of insulin secretion from human islets of Langerhans. Thus, we elucidate a pathway that converts ADCY5 gene polymorphisms into defective  $\beta$ -cell function. Since  $\beta$ -cell

decompensation is a hallmark of T2D pathogenesis irrespective of genotype, ADCY5 may provide a useful target for the restoration of insulin release in man.

**Acknowledgments.** The authors thank Drs. Tatsuya Kin and Doug O’Gorman from the Clinical Islet Isolation Laboratory in Edmonton for providing human islets for this study.

**Funding.** These studies were supported by a Diabetes UK R.D. Lawrence Research Fellowship (12/0004431) to D.J.H. and by a Wellcome Trust Senior Investigator award (WT098424AIA), a Medical Research Council Programme award (MR/J0003042/1), a Diabetes UK Project grant (11/0004210), and a Royal Society Wolfson Research Merit award to G.A.R. Isolation of human islets was supported by JDRF awards (31-2008-416) to D.B. and (31-2008-413) to L.P. (European Consortium for Islet Transplantation). P.R.J. and S.J.H. were supported by grants from the National Institute for Health Research Biomedical Research Centre, Oxford. W.-H.L. was supported by grants from the JDRF (37-2011-21) and National Institutes of Health (R01-GM-077593). The work leading to this publication has received support from the Innovative Medicines Initiative Joint Undertaking under grant 155005, resources of which are composed of financial contribution from the European Union’s Seventh Framework Programme (FP7/2007-2013), and European Federation of Pharmaceutical Industries and Associations companies’ in-kind contribution to G.A.R.

**Duality of Interest.** No potential conflicts of interest relevant to this article were reported.

**Author Contributions.** D.J.H. supervised the research, conceived and designed the study, performed the experiments, performed analysis, and wrote the manuscript with input from all authors. R.K.M. performed the experiments and analysis and conceived and designed the study. L.M. and T.J.P. performed the experiments and analysis. S.G.B. and F.S. performed the experiments. K.L.E., D.M.F.C., D.L., and W.-H.L. provided reagents. M.B., P.M., V.L., D.B., L.P., P.R.J., S.J.H., and A.M.J.S. isolated and provided human islets. G.A.R. jointly supervised the research, conceived and designed the study, performed analysis, and wrote the manuscript with input from all the authors. G.A.R. is the guarantor of this work and, as such, had full access to all the data in the study and takes responsibility for the integrity of the data and the accuracy of the data analysis.



**Prior Presentation.** Parts of this study were presented in abstract form at the 73rd Scientific Sessions of the American Diabetes Association, Chicago, IL, 21–25 June 2013.

## References

1. Scully T. Diabetes in numbers. *Nature* 2012;485:S2–S3
2. Smith U, Gale EA. Cancer and diabetes: are we ready for prime time? *Diabetologia* 2010;53:1541–1544
3. DeFronzo RA, Abdul-Ghani MA. Preservation of  $\beta$ -cell function: the key to diabetes prevention. *J Clin Endocrinol Metab* 2011;96:2354–2366
4. Rutter GA, Parton LE. The beta-cell in type 2 diabetes and in obesity. *Front Horm Res* 2008;36:118–134
5. McCulloch LJ, van de Bunt M, Braun M, Frayn KN, Clark A, Gloyn AL. GLUT2 (SLC2A2) is not the principal glucose transporter in human pancreatic beta cells: implications for understanding genetic association signals at this locus. *Mol Genet Metab* 2011;104:648–653
6. Tarasov AI, Semplici F, Ravier MA, et al. The mitochondrial  $\text{Ca}^{2+}$  uniporter MCU is essential for glucose-induced ATP increases in pancreatic  $\beta$ -cells. *PLoS ONE* 2012;7:e39722
7. Ashcroft FM, Rorsman P. ATP-sensitive  $\text{K}^{+}$  channels: a link between B-cell metabolism and insulin secretion. *Biochem Soc Trans* 1990;18:109–111
8. Grapengiesser E, Gylfe E, Hellman B. Dual effect of glucose on cytoplasmic  $\text{Ca}^{2+}$  in single pancreatic beta-cells. *Biochem Biophys Res Commun* 1988;150:419–425
9. Tsuboi T, Rutter GA. Multiple forms of “kiss-and-run” exocytosis revealed by evanescent wave microscopy. *Curr Biol* 2003;13:563–567
10. Henquin JC. Regulation of insulin secretion: a matter of phase control and amplitude modulation. *Diabetologia* 2009;52:739–751
11. Campbell JE, Drucker DJ. Pharmacology, physiology, and mechanisms of incretin hormone action. *Cell Metab* 2013;17:819–837
12. Tsuboi T, da Silva Xavier G, Holz GG, Jouaville LS, Thomas AP, Rutter GA. Glucagon-like peptide-1 mobilizes intracellular  $\text{Ca}^{2+}$  and stimulates mitochondrial ATP synthesis in pancreatic MIN6 beta-cells. *Biochem J* 2003;369:287–299
13. Shibasaki T, Sunaga Y, Fujimoto K, Kashima Y, Seino S. Interaction of ATP sensor, cAMP sensor,  $\text{Ca}^{2+}$  sensor, and voltage-dependent  $\text{Ca}^{2+}$  channel in insulin granule exocytosis. *J Biol Chem* 2004;279:7956–7961
14. Charles MA, Lawecki J, Pictet R, Grodsky GM. Insulin secretion. Interrelationships of glucose, cyclic adenosine 3:5-monophosphate, and calcium. *J Biol Chem* 1975;250:6134–6140
15. Ramos LS, Zippin JH, Kamenetsky M, Buck J, Levin LR. Glucose and GLP-1 stimulate cAMP production via distinct adenylyl cyclases in INS-1E insulinoma cells. *J Gen Physiol* 2008;132:329–338
16. McCarthy MI. Genomics, type 2 diabetes, and obesity. *N Engl J Med* 2010;363:2339–2350
17. da Silva Xavier G, Bellomo EA, McGinty JA, French PM, Rutter GA. Animal models of GWAS-identified type 2 diabetes genes. *J Diabetes Res* 2013;2013:906590
18. Dupuis J, Langenberg C, Prokopenko I, et al.; DIAGRAM Consortium; GIANT Consortium; Global BPgen Consortium; Anders Hamsten on behalf of Procardis Consortium; MAGIC investigators. New genetic loci implicated in fasting glucose homeostasis and their impact on type 2 diabetes risk. *Nat Genet* 2010;42:105–116
19. Yoshimura M, Cooper DM. Cloning and expression of a  $\text{Ca}^{2+}$ -inhibitable adenylyl cyclase from NCB-20 cells. *Proc Natl Acad Sci U S A* 1992;89:6716–6720
20. Yan L, Vatner DE, O'Connor JP, et al. Type 5 adenylyl cyclase disruption increases longevity and protects against stress. *Cell* 2007;130:247–258
21. Boesgaard TW, Grarup N, Jørgensen T, Borch-Johnsen K, Hansen T, Pedersen O; Meta-Analysis of Glucose and Insulin-Related Trait Consortium (MAGIC). Variants at DGKB/TMEM195, ADRA2A, GLIS3 and C2CD4B loci are associated with reduced glucose-stimulated beta cell function in middle-aged Danish people. *Diabetologia* 2010;53:1647–1655
22. Saxena R, Hivert MF, Langenberg C, et al.; GIANT consortium; MAGIC investigators. Genetic variation in GIPR influences the glucose and insulin responses to an oral glucose challenge. *Nat Genet* 2010;42:142–148
23. Windholz J, Kovacs P, Tönjes A, et al. Effects of genetic variants in ADCY5, GIPR, GCKR and VPS13C on early impairment of glucose and insulin metabolism in children. *PLoS ONE* 2011;6:e22101
24. Rees SD, Hydrie MZ, O'Hare JP, et al. Effects of 16 genetic variants on fasting glucose and type 2 diabetes in South Asians: ADCY5 and GLIS3 variants may predispose to type 2 diabetes. *PLoS ONE* 2011;6:e24710
25. Wagner R, Dudziak K, Herzberg-Schäfer SA, et al. Glucose-raising genetic variants in MADD and ADCY5 impair conversion of proinsulin to insulin. *PLoS ONE* 2011;6:e23639
26. Nauck MA, Homberger E, Siegel EG, et al. Incretin effects of increasing glucose loads in man calculated from venous insulin and C-peptide responses. *J Clin Endocrinol Metab* 1986;63:492–498
27. Hodson DJ, Mitchell RK, Bellomo EA, et al. Lipotoxicity disrupts incretin-regulated human  $\beta$  cell connectivity. *J Clin Invest* 2013;123:4182–4194
28. Ravier MA, Rutter GA. Isolation and culture of mouse pancreatic islets for ex vivo imaging studies with trappable or recombinant fluorescent probes. *Methods Mol Biol* 2010;633:171–184
29. Everett KL, Cooper DMF. An improved targeted cAMP sensor to study the regulation of adenylyl cyclase 8 by  $\text{Ca}^{2+}$  entry through voltage-gated channels. *PLoS ONE* 2013;8:e75942
30. He TC, Zhou S, da Costa LT, Yu J, Kinzler KW, Vogelstein B. A simplified system for generating recombinant adenoviruses. *Proc Natl Acad Sci U S A* 1998;95:2509–2514
31. da Silva Xavier G, Loder MK, McDonald A, et al. TCF7L2 regulates late events in insulin secretion from pancreatic islet beta-cells. *Diabetes* 2009;58:894–905
32. Marshall OJ. PerlPrimer: cross-platform, graphical primer design for standard, bisulphite and real-time PCR. *Bioinformatics* 2004;20:2471–2472
33. Marselli L, Thorne J, Dahiya S, et al. Gene expression profiles of Beta-cell enriched tissue obtained by laser capture microdissection from subjects with type 2 diabetes. *PLoS ONE* 2010;5:e11499
34. del Puerto A, Díaz-Hernández JL, Tapia M, et al. Adenylate cyclase 5 coordinates the action of ADP, P2Y1, P2Y13 and ATP-gated P2X7 receptors on axonal elongation. *J Cell Sci* 2012;125:176–188
35. Ravier MA, Rutter GA. Glucose or insulin, but not zinc ions, inhibit glucagon secretion from mouse pancreatic alpha-cells. *Diabetes* 2005;54:1789–1797
36. Li D, Chen S, Bellomo EA, et al. Imaging dynamic insulin release using a fluorescent zinc indicator for monitoring induced exocytotic release (ZIMIR). *Proc Natl Acad Sci U S A* 2011;108:21063–21068
37. Sanchez-Cardenas C, Fontanaud P, He Z, et al. Pituitary growth hormone network responses are sexually dimorphic and regulated by gonadal steroids in adulthood. *Proc Natl Acad Sci U S A* 2010;107:21878–21883
38. Diraison F, Parton L, Ferre P, et al. Over-expression of sterol response element binding protein-1c or culture with 5-aminoimidazole-4-carboxamide ribonucleoside induces lipogenesis and decreases glucose-stimulated insulin secretion from rat pancreatic islets. *Diabet Med* 2003;20:A77
39. Mears D, Sheppard NF Jr, Atwater I, Rojas E. Magnitude and modulation of pancreatic beta-cell gap junction electrical conductance in situ. *J Membr Biol* 1995;146:163–176
40. Hodson DJ, Schaeffer M, Romanò N, et al. Existence of long-lasting experience-dependent plasticity in endocrine cell networks. *Nat Commun* 2012;3:605DOI: 10.1038/ncomms1612.605
41. Stožer A, Gosak M, Dolensšek J, et al. Functional connectivity in islets of Langerhans from mouse pancreas tissue slices. *PLOS Comput Biol* 2013;9:e1002923
42. Onda T, Hashimoto Y, Nagai M, et al. Type-specific regulation of adenylyl cyclase. Selective pharmacological stimulation and inhibition of adenylyl cyclase isoforms. *J Biol Chem* 2001;276:47785–47793



43. Berg J, Hung YP, Yellen G. A genetically encoded fluorescent reporter of ATP:ADP ratio. *Nat Methods* 2009;6:161–166
44. Diraison F, Parton L, Ferré P, et al. Over-expression of sterol-regulatory-element-binding protein-1c (SREBP1c) in rat pancreatic islets induces lipogenesis and decreases glucose-stimulated insulin release: modulation by 5-aminoimidazole-4-carboxamide ribonucleoside (AICAR). *Biochem J* 2004;378:769–778
45. Eizirik DL, Sammeth M, Bouckennooghe T, et al. The human pancreatic islet transcriptome: expression of candidate genes for type 1 diabetes and the impact of pro-inflammatory cytokines. *PLoS Genet* 2012;8:e1002552
46. Bramswig NC, Everett LJ, Schug J, et al. Epigenomic plasticity enables human pancreatic  $\alpha$  to  $\beta$  cell reprogramming. *J Clin Invest* 2013;123:1275–1284
47. Parton LE, McMillen PJ, Shen Y, et al. Limited role for SREBP-1c in defective glucose-induced insulin secretion from Zucker diabetic fatty rat islets: a functional and gene profiling analysis. *Am J Physiol Endocrinol Metab* 2006;291:E982–E994
48. Bosco D, Armanet M, Morel P, et al. Unique arrangement of alpha- and beta-cells in human islets of Langerhans. *Diabetes* 2010;59:1202–1210
49. Elayat AA, el-Nagggar MM, Tahir M. An immunocytochemical and morphometric study of the rat pancreatic islets. *J Anat* 1995;186:629–637
50. Roger B, Papin J, Vacher P, et al. Adenylyl cyclase 8 is central to glucagon-like peptide 1 signalling and effects of chronically elevated glucose in rat and human pancreatic beta cells. *Diabetologia* 2011;54:390–402
51. Willoughby D, Cooper DM. Organization and  $\text{Ca}^{2+}$  regulation of adenylyl cyclases in cAMP microdomains. *Physiol Rev* 2007;87:965–1010
52. Rutter GA, Tsuboi T, Ravier MA.  $\text{Ca}^{2+}$  microdomains and the control of insulin secretion. *Cell Calcium* 2006;40:539–551
53. Dyachok O, Isakov Y, Sâgetorp J, Tengholm A. Oscillations of cyclic AMP in hormone-stimulated insulin-secreting beta-cells. *Nature* 2006;439:349–352
54. Marchetti P, Lupi R, Bugliani M, et al. A local glucagon-like peptide 1 (GLP-1) system in human pancreatic islets. *Diabetologia* 2012;55:3262–3272
55. Holz GG. Epac: A new cAMP-binding protein in support of glucagon-like peptide-1 receptor-mediated signal transduction in the pancreatic beta-cell. *Diabetes* 2004;53:5–13
56. Miki T, Minami K, Shinozaki H, et al. Distinct effects of glucose-dependent insulinotropic polypeptide and glucagon-like peptide-1 on insulin secretion and gut motility. *Diabetes* 2005;54:1056–1063